Characterization of nuclear ferritin and mechanism of translocation

Nodar SURGULADZE*, Stephanie PATTON*, Anna COZZI†, Michael G. FRIED‡ and James R. CONNOR*[1]

*Department of Neurosurgery, The Pennsylvania State University College of Medicine, 500 University Drive, Hershey, PA 17033, U.S.A., †Biological and Technological Research Department, Istituto di Ricovero e Cura a Carattere Scientifico, H. San Raffaele, Via Olgettina 58, 20132 Milan, Italy, and ‡Department of Molecular and Cellular Biochemistry, University of Kentucky, MS 607A Medical Science Building, Lexington, KY 40536-0298, U.S.A.

Ferritin, normally considered a cytoplasmic iron-storage protein, is also found in cell nuclei. It is an established fact that H-ferritin is the major form of nuclear ferritin, but little is known about the roles of ferritin in nuclei or about the mechanisms that control its appearance within the nuclear volume. In the present study, we show that, for human SW1088 astrocytoma cells, the nuclear and cytoplasmic forms of H-ferritin are products of the same mRNA. Histochemical and biochemical evidence is presented showing that ferritin is distributed non-randomly within the nuclear volume and that it preferentially associates with heterochromatin. Both cytoplasmic and nuclear populations of H-ferritin contain mixtures of non- and O-glycosylated forms, but the nuclear population is enriched in O-glycosylated forms. Cells treated with alloxan, a potent inhibitor of O-glycosylation, contained significantly less nuclear ferritin compared with cells grown in control media. Alloxan inhibited the reappearance of H-ferritin in nuclei of cells released from conditions of iron depletion, but did not prevent its disappearance from nuclei of cells undergoing iron depletion. These results suggest that O-glycosylation accompanies the transfer of ferritin from the cytoplasm to the nucleus, but does not influence the reverse process. The picture that emerges is one in which ferritin translocation between the cytoplasm and the nucleus is post-translationally regulated and responds to environmental and nutritional cues.

Key words: alloxan, desferoxamine, nuclear ferritin, nuclear localization signal, O-glycosylation, translocation.

INTRODUCTION

Ferritin has been investigated for decades as a cytosolic iron-storage protein, a plasma protein, an indicator of the level of body-iron storage and a prognostic indicator of some cancers. Recent studies have shown that the intracellular distribution of ferritin is subcompartmentalized to the nuclei and mitochondria [1,2]. Most of the initial observations of intranuclear ferritin have been associated with the supraphysiological conditions subsequent to iron overload in mice, rats and baboons or associated with a pathological condition such as pigmentary cirrhosis and chronic progressive motor disturbance [3–8]. The cell types in which intranuclear ferritin has been described in these latter conditions include hepatocytes, bone-marrow macrophages, reticular cells and muscle and nerve cells. Nuclear ferritin has also been observed in some brain tumour cells and glial cell lines in culture [9,10]. In normal tissues, avian corneal endothelial cells [11] and neurons of the rat and pig brains [12–15] transiently express nuclear ferritin during development. The presence of ferritin in neuronal cell nuclei can be prolonged by exposing animals during development to hypoxic/ischaemic challenge [14]. In cell-culture models, the amount of ferritin in cell nuclei can be modified by changes in iron status or by exposure to inflammatory cytokines and/or oxidative stress [10]. In all cases, the major form of ferritin in the cell nuclei is the H-subunit.

Experimentally, microinjection of ferritin into the cytoplasm of most cells resulted in the retention of the molecule within the cytoplasm [12,13]. In some cells, however, ferritin could enter the nucleus, although it did so less efficiently compared with low-molecular-mass proteins [16]. If the microinjected ferritin is conjugated with a synthetic peptide containing the basic NLS (nuclear localization signal) of simian-virus-40 large T-antigen, efficient translocation to the nucleus can be observed [13]. However, the existence of neither an NLS nor any other sequence that promotes nuclear translocation (such as the M9 signal [15]) has been detected on ferritin. Analyses with deletion constructs for ferritin [17] failed to detect any discrete region that might function as a non-consensus NLS. Transfection analyses using myc-tagged ferritin deletion constructs in corneal epithelial cells showed that, for nuclear transport in corneal epithelial cells, more than 83 % of the ferritin H chain must be intact. Thus there seems to be no specific region that serves as an NLS. We have shown that, for exogenously applied H-ferritin to enter the nuclei of astrocytoma cells in culture, the cells should first be treated with an iron chelator and permeabilized. A mutant form of ferritin that does not have ferroxidase activity can also enter the nucleus under similar conditions, indicating that the iron-uptake activity of ferritin does not dictate nuclear translocation [10]. L-ferritin is not translocated to the nucleus, indicating a specific pathway for H-ferritin [10]. A ferritin chaperone referred to as a 'ferrotoid' that may mediate nuclear translocation has been described, but it appears to be specific to avian corneal epithelial cells [18] and thus may not account for the increasing number of cells in which ferritin nuclear translocation has been observed. Additional factors that regulate H-ferritin transfer between the cytoplasm and nucleus are addressed in the present study.

Investigation of the function(s) of nuclear ferritins is currently underway. Nuclear ferritin has been shown to protect DNA from UV-induced damage in avian corneal epithelial cells [8]. In other experimental systems, its function may be more complex. We

Abbreviations used: AEBSF, 4-(2-aminoethyl)benzenesulphonyl fluoride; DAPI, 4,6-diamidino-2-phenylindole; DFO, desferoxamine; DMEM, Dulbecco's modified Eagle's medium; DTT, dithiothreitol; E-64, *trans*-epoxysuccinyl-L-leucylamido-(4-guanidino)butane; FAC, ferric ammonium citrate; LDH, lactate dehydrogenase; MTT, 3-(4,5-dimethylthiazol-2-yl)-2,5-diphenyl-2*H*-tetrazolium bromide; NLS, nuclear localization signal; *O*-GlcNAc, *O*-linked *N*-acetylglucosamine; siRNA, small interfering RNA.

[1] To whom correspondence should be addressed, at G.M. Leader Family Laboratory for Alzheimer's Disease, M.S. Hershey Medical Center, Penn State University College of Medicine, Hershey, PA 17033, U.S.A. (email jrc3@psu.edu).

have shown that a brief incubation of iron with ferritin decreases the rate of iron-dependent DNA damage [10], whereas prolonged exposure of DNA to ferritin results in DNA nicking at rates that depend on the iron content of the protein [19]. Although DNA nicking is believed to be deleterious to cell survival, it remains possible that cycles of DNA nicking and repair will play a role in relaxing the torsional stresses brought about by transcription, replication and chromatin remodelling. It has also been proposed that ferritin can act as a source of iron for iron-dependent enzymatic functions or structures [18,20–22]. These possible roles for nuclear ferritin are supported by the observation that it is present in developing tissues and in rapidly growing tumours [10], that it can be chemically cross-linked to DNA in live astrocytoma cells [10] and that it binds DNA *in vitro* [10,19,23,24].

In the present study, we attempt to answer a number of questions about the presence of H-ferritin in the nuclei of human astrocytoma cells. These include: are nuclear and cytoplasmic H-ferritins, products of the same genes? What processes regulate the movement of ferritin between the cytoplasm and nucleus? Is there a difference between H- and L-ferritins that may elucidate why the H-subunit is translocated preferentially? Finally, how is ferritin distributed within the nuclear volume? The answers would provide clues to the dynamics and functions of nuclear ferritins.

MATERIALS AND METHODS

Reagents and antibiotics

DFO (desferoxamine), alloxan, the vital stain azure C, DAPI (4,6-diamidino-2-phenylindole), L-glutamine and the protease inhibitors AEBSF [4-(2-aminoethyl)benzenesulphonyl fluoride], aprotinin, leupeptin, bestatin, pepstatin and E-64 [*trans*-epoxysuccinyl-L-leucylamido-(4-guanidino)butane] were obtained from Sigma. Penicillin, streptomycin and trypsin were from Gibco BRL (Gaithersburg, MD, U.S.A.). All other biochemicals were of the reagent grade.

Cell culture

Human astrocytoma SW1088 cells (A.T.C.C., Manassas, VA, U.S.A.) were cultured in supplemented DMEM [Dulbecco's modified Eagle's medium supplemented with 10 % (v/v) fetal calf serum (Biocell, Cardiff, U.K.), 4 mM L-glutamine, 100 units/ml penicillin and 1 ng/ml streptomycin]. Cultures were maintained in 150 mm culture flasks and passaged every 7 days.

Cell viability assay

Cell viability measurement was performed using the reagent 3-(4,5-dimethylthiazol-2-yl)-2,5-diphenyl-2*H*-tetrazolium bromide (MTT) [25], obtained from Roche Applied Science (Indianapolis, IN, U.S.A.). The assay was performed according to the manufacturer's instructions.

DFO and alloxan treatments

The iron chelator DFO was used to examine the effect of iron chelation on ferritin localization in the nuclei of astrocytoma cells. Cells were cultured in the presence of 100 μM DFO for 72 h. Alloxan, an inhibitor of O-glycosylation, was used in astrocytoma cell cultures at final concentrations of 0.1 and 1.0 mM. Six cultures were established in parallel and allowed to reach 80 % confluence. The first three were treated with 100 μM DFO for 72 h, then rinsed in Hanks balanced salt solution to remove the free DFO and returned to standard medium alone or to a medium containing 0.1 mM FAC (ferric ammonium citrate) or 0.1 mM DFO. After these treatments, culturing was continued for 24 h. Another set of three cultures were treated with 100 μM DFO + 1 mM alloxan for 72 h. The cells were rinsed in Hanks balanced salt solution to remove free reagents and returned to standard medium containing 1 mM alloxan or a medium containing 0.1 mM FAC + 0.1 mM alloxan or a medium containing 100 μM DFO + 1 mM alloxan. After these treatments, the culturing was continued for 24 h. At the end of the culture period, cells were harvested and nuclear and cytosolic fractions were prepared as described below.

Nuclear and cytosolic fractions

Plated astrocytoma cells were rinsed in Hanks balanced salts, trypsinized and the cells were collected by centrifugation (800 ***g*** for 10 min). The pelleted cells were rinsed twice in ice-cold PBS buffer [0.01 M sodium phosphate (pH 7.4 at 25 °C), 138 mM NaCl and 2.7 mM KCl] and collected by centrifugation. The cell pellets were resuspended in 20 vol. of 10 mM Hepes (pH 7.9 at 25 °C), 1.5 mM $MgCl_2$, 10 mM NaCl and 0.5 mM DTT (dithiothreitol) containing the following protease inhibitors: AEBSF (1 mM), aprotinin (0.8 μM), leupeptin (20 μM), bestatin (40 μM), pepstatin (15 μM) and E-64 (14 μM). Cell suspensions were incubated in ice for 30 min and collected by centrifugation. The pelleted cells were resuspended in 10 vol. of 10 mM Hepes (pH 7.9 at 25 °C), 1.5 mM $MgCl_2$, 10 mM NaCl and 0.5 mM DTT containing 0.5 % Nonidet P40 and homogenized gently using a Dounce homogenizer. Cell lysis was verified by light microscopy. Nuclei were collected by centrifugation at 1000 ***g*** for 10 min. The supernatant was collected for cytosolic analysis. Crude nuclei were resuspended by gentle homogenization in 0.88 M sucrose and 3 mM $MgCl_2$ and centrifuged at 2500 ***g*** for 20 min to remove cell debris. The pellet was collected, resuspended in the buffer appropriate for nucleoli, nuclear matrix or soluble chromatin preparation (see below) and stored at − 80 °C until use. Assay for the cytoplasmic marker enzyme LDH (lactate dehydrogenase) was performed on all nuclear fractions to determine cytoplasmic contamination [26]. On the basis of the very low activities observed in these assays, we estimate that $\leqslant$ 1 % of the proteins in our nuclear preparations consisted of contaminants from the cytoplasm.

Soluble nuclear fraction

Isolated nuclei were washed once with 0.1 mM PBS containing 0.1 % Triton X-100 and resuspended in hypo-osmotic 10 mM Hepes (pH 7.0), 150 mM sucrose and 10 mM NaCl. The resulting suspension was centrifuged for 10 min at 3000 ***g***. The supernatant was retained as a soluble nuclear fraction.

Digestion with nuclease

Isolated nuclei were washed once with 0.1 mM PBS containing 0.1 % Triton X-100 and resuspended in 10 mM Hepes (pH 7.0), 150 mM sucrose, 10 mM NaCl and 1.5 mM $MgCl_2$. Digestion with DNase I (100 units/μg of nucleic acid) or DNase I + RNase A (1 unit/μg of nucleic acid) was performed at 37 °C for 10 min. The resulting suspension was centrifuged for 10 min at 3000 ***g***. The supernatant was retained as a nuclease-digested soluble nuclear fraction.

Nuclear matrix

Isolated nuclei were washed once with 0.1 mM PBS containing 0.1 % Triton X-100 and resuspended in 10 mM Hepes (pH 7.0), 150 mM sucrose, 50 mM NaCl and 3 mM $MgCl_2$ for digestion with DNase I (100 units/μg of DNA). Digestion was performed at

Table 1 Sequences of double-stranded siRNAs used to suppress H-ferritin translation

siRNA	Sequence
H-siRNA1 (beginning 29 nt downstream of start codon)	5′-GCCAGAACUACCACCAGGAC-3′ 3′-CGGUCUUGAUGGUGGUCCUG-5′
H-siRNA2 (beginning 129 nt downstream of start codon)	5′-GUGGCUUUGAAGAACUUUGC-3′ 3′-CACCGAAACUUCUUGAAACG-5′
H-siRNA3 (beginning 333 nt downstream of start codon)	5′-GAAUCAGUCACUACUGGAAC 3′ 3′-CUUAGUCUGUGAUGACCUUG-5′
H-siRNA4 (beginning 501 nt downstream of start codon)	5′-GGAAUAUCUCUUUGACAAGC-3′ 3′-CCUUAUAGAGAAACUGUUCG-5′

37 °C for 10 min. Nuclei were collected by centrifugation at 800 ***g*** for 10 min at 4 °C and suspended in high-salt-containing buffer at 4 °C in 10 mM Hepes (pH 7.4 at 4 °C), 2 M NaCl, 1 mM EGTA and 300 mM sucrose. The nuclease-resistant matrix fraction was collected by centrifugation at 10 000 ***g*** for 15 min.

Nucleoli

Isolated nuclei were suspended by gentle homogenization in 0.34 M sucrose and 0.5 mM $MgCl_2$, transferred to an ice-cold sonicator rosette and sonicated (10×10 s bursts followed by 20 s cooling periods). The release of nucleoli was monitored by microscopic examination and staining with Azure C [27]. Sonicated fractions were underlayered with 5 vol. of 0.88 M sucrose and centrifuged at 3000 ***g*** for 20 min. The pellet contained isolated nucleoli.

Production of siRNAs (small interfering RNAs)

Generation and purification of the double-stranded siRNAs has been described previously [28]. The sequences used in the present study are shown in Table 1. Anti-sense siRNAs were obtained from Qiagen (Chatsworth, CA, U.S.A.) for use as experimental controls.

Proteins and antibodies

The H-ferritin-specific antibodies (rHO2 and HS-59) and recombinant H-ferritin (rH-ferritin) used in the present study have been described previously [29–32]. Polyclonal anti-human ferritin antibody (special order, Quality Controlled Biochemicals, Hopkinton, MA, U.S.A.) and human liver ferritin (lot no. 23) were purchased from ICN (Aurora, OH, U.S.A.). A monoclonal antibody raised against *O*-GlcNAc (O-linked *N*-acetylglucosamine) was purchased from Covance and Alexa 488-conjugated goat anti-mouse IgG was from Molecular Probes.

Cell transfection, immunofluorescence and confocal microscopy

Double-stranded siRNAs (1.4 μg) were transfected into 2×10^6 SW1088 cells using the Amaxa Rat Astrocyte Nucleofector™ kit (Amaxa, Gaithersburg, MD, U.S.A.) according to the manufacturer's instructions. The resulting cells were grown in DMEM (Gibco BRL), 10 % (v/v) fetal bovine serum (ClonTech Laboratories, Palo Alto, CA, U.S.A.), 100 units/ml penicillin, 100 μg/ml streptomycin and 1 mM L-glutamine. Cells were harvested at approx. 80 % confluency. Analysis of a parallel control transfection of these cells, with the pc3.1-GFP (where GFP stands for green fluorescent protein) construct (provided by Amaxa), showed that approx. 75 % of the cells were transfected. As a negative control, SW1088 cells were mock-transfected under the same conditions using water in place of the siRNA solution.

As a further test of transfection efficiency and as a control for non-specific effects of the transfection procedure, SW1088 cells were transfected with a rhodamine-conjugated non-specific siRNA (obtained from Qiagen). After 24 h in culture, cells were harvested and suspended in an equal volume of lysis buffer [20 mM Hepes (pH 7.4 at 21 °C), 4 % (w/v) SDS, 20 mM DTT, 1 mM AEBSF, 0.8 μM aprotinin, 20 μM leupeptin, 40 μM bestatin, 15 μM pepstatin and 14 μM E-64]. Cells were sonicated for 10 s on ice, protein concentrations were measured and ferritin contents were detected by Western blotting using an anti-human H-ferritin monoclonal antibody (HS-59; a gift from Dr P. Arosio, University of Milan, Milan, Italy).

After transfection, approx. 5×10^4 cells were plated on untreated glass slips. Cells were allowed to attach for 1 h at 37 °C under a 5 % humid CO_2 atmosphere; subsequently, the slips were submerged in supplemented DMEM and cultured at 37 °C under a 5 % humid CO_2 atmosphere. At 24 h intervals, slips were removed, washed three times with PBS and fixed in ice-cold acetone for 3 min. The slips were incubated for 2 h at room temperature (21 °C) with 10 % (v/v) normal goat serum (Vector Laboratories, Burlingame, CA, U.S.A.) to block non-specific interactions; the slips were then incubated with primary anti-H monoclonal (rH02) or polyclonal antibodies (in 5 % normal goat serum) for 90 min at room temperature. Free antibodies were removed by three washes with PBS and the slips were then incubated with Alexa-conjugated goat anti-mouse or, where appropriate, anti-rabbit secondary antibody and DAPI for a further 60 min. After three washes with PBS, slips were mounted and covered with a coverslip. Negative controls for antibody staining were obtained by preparing the slips as described above, but omitting the primary antibody. Confocal microscopy was performed using a Leica TCS equipped with a DMR inverted microscope and a $\times 63/1.4$ NA objective. An argon/krypton laser was used to generate light at 488 nm for Alexa excitation and 360 nm for DAPI excitation. A high-pass filter with a wavelength cutoff at 500 nm was used to recover Alexa fluorescence and a low-pass filter with wavelength cutoff at 460 nm was used to detect DAPI fluorescence. Each fluorophore was excited sequentially to achieve the lowest interference between the two detector channels.

Fluorimetric analysis

Digital pictures were taken at $\times 10$ magnification with a 2-s aperture using a Cooke Sensicam digital camera to obtain a baseline level of fluorescence. For each time period, three different slips were examined and, within each slip, multiple ($\geqslant 3$) microscopic fields were captured for analysis. Nuclear ferritin content was analysed on the basis of the fluorescence intensities of the entire nuclear regions. Images were analysed for mean density pixel counts per bright object with ImagePro 4.5 software (Phase Imaging Systems, Glen Mills, PA, U.S.A.). Background fluorescence was determined and subtracted from each image [33,34]. The results are presented normalized to a control value obtained with nuclei subjected to mock transfection using a buffer instead of siRNA.

Immunoprecipitation and Western-blot analyses

Cell lysate samples (1 ml, ~ 500 μg of protein) were incubated with 20 μl of Protein A/G–agarose beads (Pierce, Rockford, IL, U.S.A.) for 1 h and then centrifuged at 800 ***g*** for 3 min at 4 °C. Supernatants were collected and incubated with a polyclonal antibody raised against human ferritin or against the *O*-glucosyl-moiety for 2 h at 4 °C. A further 20 μl of Protein A/G–agarose beads was then added and the mixture was incubated overnight

at 4 °C. The pellets were collected by centrifugation at 800 ***g*** for 5 min at 4 °C and washed by suspension in PBS buffer followed by centrifugation. This procedure was repeated four times. Pellets were then suspended in SDS-gel loading buffer, boiled for 5 min and analysed by SDS/PAGE. After electrophoresis, proteins were transferred on to 0.2 μm nitrocellulose membranes using a Bio-Rad Trans-Blot apparatus. Membranes were incubated overnight with solutions of HS-59 mouse anti-rH-ferritin antibody or rabbit anti-human ferritin polyclonal antibody at 1:1500 dilution. Immunocomplexes were detected using peroxidase-conjugated goat anti-mouse or anti-rabbit IgGs (Sigma), visualized with the ECL+ kit (Amersham Biosciences, Piscataway, NJ, U.S.A.). Images were captured using Blue Bio Film (Denville Scientific, Metuchen, NJ, U.S.A.). Relative amounts of immunoproducts were estimated by film densitometry using ImageQuant™ software (Molecular Dynamics, Sunnyvale, CA, U.S.A.) as described by Surguladze et al. [19].

Detection of glycosylated proteins

SW1088 cultures were treated with different concentrations of alloxan for 96 h. At the end of the culture period, cells were harvested, resuspended in an equal volume of lysis in buffer and sonicated for 10 s on ice, as described above. Protein concentrations were measured and aliquots containing 1, 5 and 10 μg of total cell proteins were applied in triplicate to a 0.2 μm nitrocellulose membrane (Amersham Biosciences). Membranes were blocked by incubating for 1 h at 21 $\pm$ 1 °C with 5 % blotto and then incubated overnight with solutions of monoclonal anti-GlcNAc antibody at 1:1000 dilution. Immunocomplexes were detected using peroxidase-conjugated goat anti-mouse IgG (Sigma) and visualized with the ECL+ kit (Amersham Biosciences). Images were captured using Blue Bio Film (Denville Scientific). Relative amounts of the immunoproducts were estimated by film densitometry using ImageQuant™ software (Molecular Dynamics) by the method of Surguladze et al. [19].

Supercoil relaxation assay

DNA backbone breakage was detected using a superhelical DNA relaxation assay [35,36]. The reaction mixtures (30 μl) contained covalently closed circular pUC19 DNA (0.5 μg; Sigma) dissolved in 10 mM Hepes (pH 7.5), 50 mM NaCl, 2.5 mM $MgCl_2$ and 2.5 mM DTT. This particular preparation of DNA has a range of superhelical densities that allow the resolution of topoisomers under our standard electrophoresis conditions, in the absence of added ethidium bromide. With other preparations, only a single band (representing the ensemble of closed-circular topoisomers) and one band representing the relaxed form are resolved. Reactions were initiated by the addition of recombinant human H-ferritin (rH-ferritin). After timed incubations, reactions were terminated by the addition of 0.1 vol. of 50 % (v/v) glycerol, 50 mM EDTA and 0.1 % Bromophenol Blue. Samples were subjected to electrophoresis on 1.5 % (w/v) agarose gels [37]. The mole fractions of superhelical and relaxed forms were measured by densitometry of photographic negatives of the gels after staining with 0.5 μg/ml ethidium bromide [19].

RESULTS

Ferritin is unevenly distributed within the nuclear volume

We have used confocal microscopy to evaluate the intranuclear distribution of ferritin in cultured astrocytoma cells (Figure 1). Optical thin slices through cells stained with Alexa-labelled anti-ferritin antibody and counterstained with DAPI reveal that ferritin is present in both nuclear and perinuclear regions. In both compartments, the distribution of ferritin appears to be non-uniform, with discrete regions of intense staining, surrounded by regions with almost no staining. Within the nuclear volume, the size of the intensely stained regions is highly variable, ranging from nearly 1 μm down to the limit of detection. There is no immunocytochemically detectable L-ferritin in the cell nuclei (results not shown).

The non-uniform distribution of H-ferritin might be due to its association with a particular nuclear component. Fractionation studies were therefore performed to determine the distribution of ferritin between bulk chromatin (solubilized with DNase I), nucleoli and nuclear matrix. Cultured SW1088 cells, previously shown to contain nuclear ferritin [10], were used for these studies. The cytoplasmic enzyme LDH was assayed to detect contamination by cytoplasmic components. The nuclear preparations used in these studies contained $\leqslant$ 1 % of the LDH activity of cytoplasmic fractions.

Relative to total protein, the highest amount of ferritin was found in soluble nuclear fractions, an intermediate quantity was found in the nuclear matrix and the smallest amount was found in nucleoli (Figure 2A). The non-uniform distribution of ferritin in these fractions is consistent with the pattern of nuclear staining described above and suggests that H-ferritin may be preferentially associated with one or more components of heterochromatin.

Ferritin release is not enhanced by DNase action

Several lines of evidence indicate that some forms of H-ferritin but not L-ferritin are capable of binding DNA [19,23,38]. We reasoned that if ferritin interacts preferentially with exposed DNA or with extended chromatin regions, it should be preferentially released by the action of DNase I. A test of this prediction is shown in Figure 2(A). When nuclei were subjected to protein extraction with and without DNase I, the inclusion of DNase did not increase the concentration of ferritin present in the soluble fraction as detected by immunoblotting. This result suggests that ferritin may not be preferentially associated with DNase I-sensitive structures or that any association is too labile to be detected by these methods. The dynamic nature of ferritin–DNA interactions *in vitro* [10,19] is consistent with the latter view.

The ferritin that is present in SW1088 nuclei appears to exist in several covalent states (Figure 2B). SDS/PAGE analysis with Western-blot detection shows that approx. 85 % of the molecules migrated with a relative molecular mass M_r of approx. 22 000, consistent with the monomer molecular mass of human H ferritin deduced from the sequence (M_r 21 094). Approximately 10 % of the protein had an M_r of 45 000, suggesting the presence of covalent subunit dimers. The remainder ($\sim$5 %) migrated more slowly, suggesting the presence of even more subunit multimers. L-ferritin was not detected in the SDS/PAGE analysis consistent with the immunocytochemical results.

Nuclear and cytoplasmic H-ferritins appear to be products of the same gene

The results presented above demonstrate the presence of a ferritin-like nuclear protein of appropriate molecular mass ($M_r \sim 21\,000$) that reacts efficiently with mouse and rabbit anti-human H-ferritin antibodies. Other experiments indicate that this protein resists thermal denaturation and attack by proteinase K in a manner that is characteristic of cytoplasmic ferritin (results not shown). However, these results do not establish that the nuclear protein

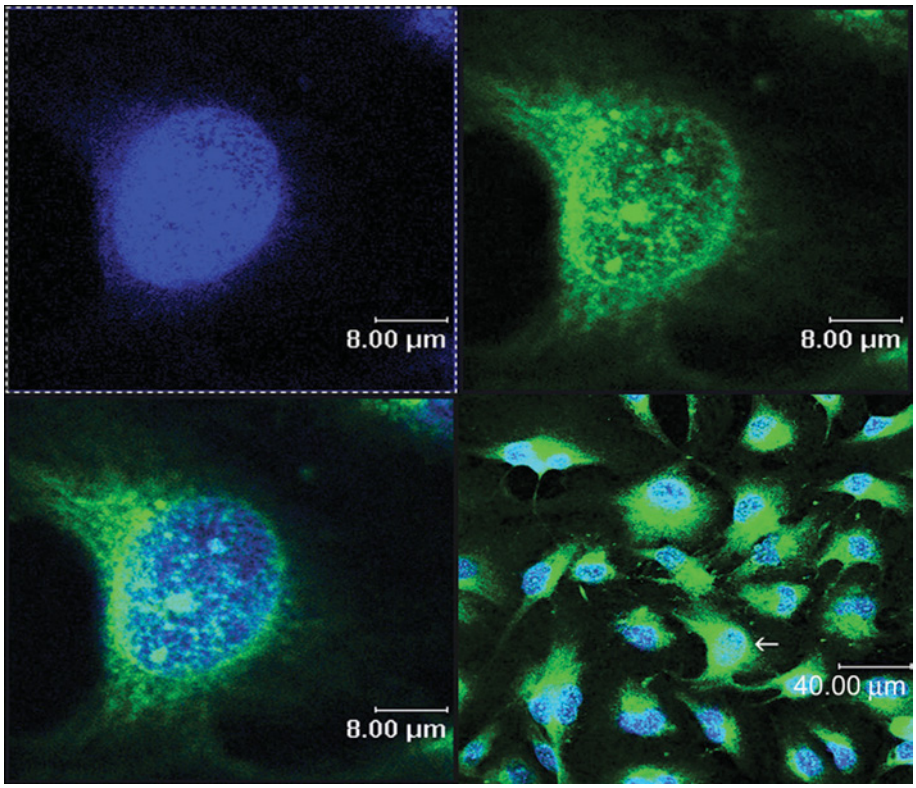

Figure 1 Confocal image of SW1088 cells

Human grade III astrocytoma cells (SW1088) were fixed, and incubated with polyclonal rabbit anti-human H-ferritin antibody at 1:200 dilution, followed by Alexa 488-conjugated goat anti-rabbit IgG at 1:200 dilution. Nuclei were visualized by DAPI staining at a final concentration of 100 ng/ml. Slips were processed as described in the Materials and methods section. Alexa- and DAPI-fluorescence emissions (shown in green and blue respectively) were observed using a confocal microscope with illumination at 488 nm (Alexa) and 360 nm (DAPI).

is identical with the cytoplasmic form of ferritin. To determine whether the nuclear and cytoplasmic forms of ferritin are products of a common gene, siRNA inhibition of translation was performed. siRNAs were prepared against DNA sequences encoding cytoplasmic H-ferritin (Table 1). These were transfected into SW1088 cells and the relative ferritin concentrations in nuclear and cytoplasmic compartments were determined as a function of time after transfection. As shown in Figure 3(A), the H-ferritin nuclear signal was significantly decreased within 48 h of transfection with H-ferritin siRNA. The relative amount of nuclear ferritin continued to decrease until 72 h after transfection, after which the signal gradually returned to normal by the 144 h time point. Cells transfected with a non-specific RNA showed no decrease in ferritin (Figure 3B). Taken together, these results suggest that both nuclear and cytoplasmic H-ferritins are products of the same gene.

The siRNA-dependent changes in cytoplasmic ferritin concentration are mirrored by those in the nucleus, although the changes in nuclear concentration take place with an approx. 16 h delay. This delay suggests that nuclear ferritin concentrations depend on those in the cytoplasm and is consistent with models in which ferritin is synthesized in the cytoplasm and subsequently transferred to the nucleus.

Detection of glycosylated H-ferritin

If the cytoplasmic and nuclear forms of H-ferritin are products of the same gene, what regulates the distribution of the protein between nuclear and cytoplasmic compartments? One possibility is O-glycosylation [39–44]. Analysis of the H-ferritin sequence using the program YinOYang 1.2 (Center for Biological Sequence Analysis, Technical University of Denmark; available at http://www.cbs.dtu.dk/researchgroups/protfunction.php) predicts the existence of six sites for O-glycosylation, whereas the sequence of L-ferritin (which appears to be restricted to the cytoplasm) has only one site for O-glycosylation (Table 2). To determine whether nuclear and cytoplasmic H-ferritins differ in O-glycosylation, fractions were isolated from SW1088 cells and subjected to immunoprecipitation using antibodies raised against *O*-GlcNAc. The immunoprecipitated proteins were analysed by PAGE and Western blotting using a polyclonal H-ferritin antibody as the detection reagent (Figure 4). Strong signals with electrophoretic mobilities consistent with $M_r \sim 22\,000$ support our conclusion that *O*-GlcNAc-H-ferritin is present in both nuclear and cytoplasmic fractions.

Inhibition of O-glycosylation also inhibits translocation of H-ferritin

To determine whether the O-linked glycosylation was functionally involved in ferritin nuclear translocation, cells were treated with alloxan, a strong inhibitor of O-linked glycosylation [45]. As demonstrated previously, SW1088 cells contain nuclear ferritin under resting conditions [10]. Therefore to study the effect of alloxan on ferritin translocation, we first treated the cells with the iron chelator DFO to decrease the amount of nuclear ferritin. Cells were cultured for 3 days either in normal medium supplemented with 100 μM DFO or in 100 μM DFO + 1 mM alloxan. After this initial growth period, the cells cultured with DFO alone were grown for 72 h in either fresh medium, a medium supplemented with 100 μM DFO or a medium supplemented with 100 μM FAC.

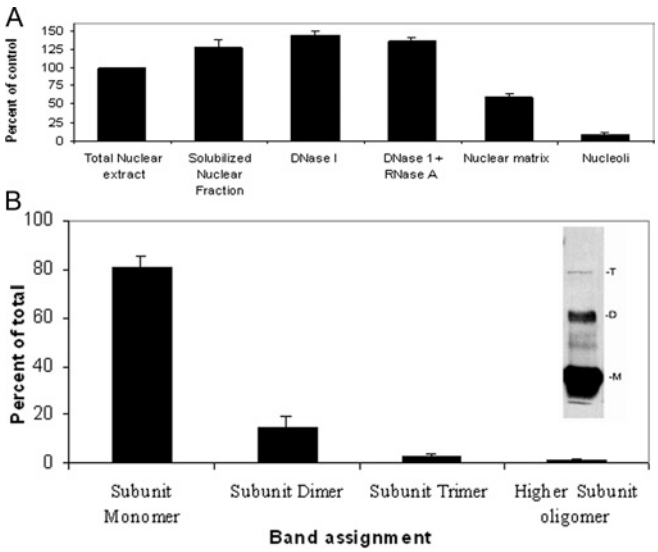

Figure 2 Distribution of ferritin in subnuclear fractions and oligomerization of nuclear ferritin

(**A**) Total nuclear extract and different fractions (soluble nuclear fraction, nuclease-digested fractions, nuclear matrix and nucleoli) were prepared as described in the Materials and methods section. Samples containing 20 μg of protein were resolved by SDS/PAGE and ferritin contents were detected by Western blotting using the HS-59 mouse anti-rH-ferritin antibody as a probe. Immunocomplexes were detected using peroxidase-conjugated goat anti-mouse IgG. Images were captured on a film and relative band intensities were estimated by densitometry. The results are presented as band intensities normalized to that of the unfractionated nuclear sample. The error bars represent S.D. values for triplicate samples obtained from independent cell preparations. (**B**) Total nuclear extract (20 μg of protein/sample) was resolved by SDS/PAGE. Ferritin was detected by Western blotting using HS-59 mouse anti-rH-ferritin antibody as described in the Materials and methods section. The intensities of bands with mobilities corresponding to the monomeric subunit of ferritin (M_r 21094) and subunit dimers, subunit trimers and higher subunit oligomers are represented as a percentage of the summed band intensities. Increasing the concentrations of SDS and 2-mercaptoethanol (up to 4% and 7 mM respectively) as well as increasing the sample boiling time did not change the ratio of different multimers. Increasing the concentrations of SDS and 2-mercaptoethanol (up to 4% and 7 mM respectively) as well as increasing the sample boiling time did not change the ratio of different multimers. The inset shows a representative gel lane with bands designated M (subunit monomer), D (subunit dimer) and T (subunit trimer). An additional, faint band with mobility intermediate to that of ferritin subunit monomer and subunit dimer is regularly seen. At present, we do not know the identity of this species. The error bars represent S.D. values for three independent samples.

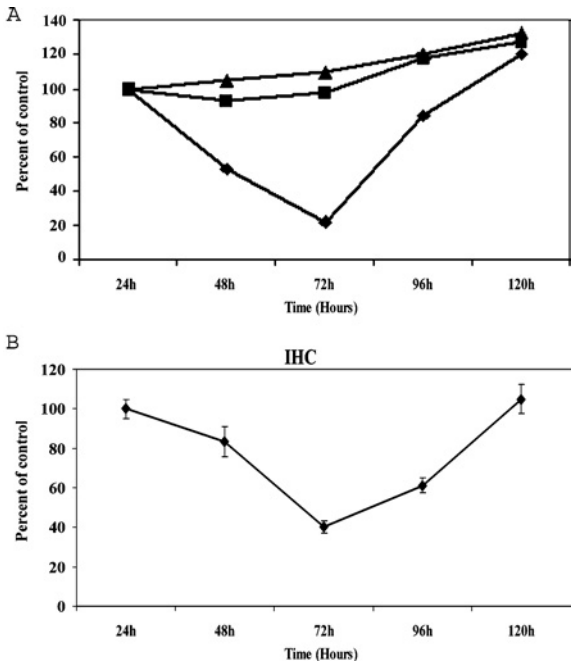

Figure 3 Nuclear and cytoplasmic H-ferritins are translated from the same mRNA

SW1088 cells were transfected with anti-H-ferritin siRNA as described in the Materials and methods section. The cells were transfected and then plated in flasks (Western-blot analysis) or on coverslips (for immunohistochemical analysis). The data from Western-blot analysis are shown in (**A**). Cells for biochemical analysis were suspended, lysed and the relative ferritin contents of whole cell extracts were determined at the indicated times by Western blotting as described in the Materials and methods section. Results are expressed as band intensities normalized to the ferritin content of the parent, untransfected SW1088 cells, sampled at the time of transfection. ■, cells transfected with siRNA against human H-ferritin; ▲, cells transfected with non-specific RNA; ◆, cells exposed to mock transfection using a buffer instead of RNA solution. For the immunohistochemical analysis (**B**), the cells were fixed and immunostained for H-ferritin as described in the Materials and methods section at the indicated times. For each time period, three different slips were examined and, within each slip, multiple ($\geqslant$3) microscopic fields were captured for analysis. Nuclear ferritin content was analysed on the basis of the fluorescence intensities of entire nuclear regions. The results are presented normalized to a control value obtained with nuclei subjected to mock transfection using buffer instead of siRNA. The transfection efficiency was determined to be $\geqslant$90% using rhodamine-conjugated non-specific RNA. In both (**A**) and (**B**), the error bars represent S.D. values. The similar pattern of decrease in nuclear and whole-cell H-ferritin contents after transfection with siRNA indicates that nuclear and cytoplasmic H-ferritins are expressed from the same message.

The cells initially cultured in the presence of DFO and alloxan were grown for 72 h in fresh medium containing 1 mM alloxan, in fresh medium supplemented with 100 μM DFO + 1 mM alloxan or in fresh medium supplemented with 100 μM FAC + 1 mM alloxan. This experimental procedure is schematically represented in Figure 5(A). In experiments in which cells were treated with DFO in the absence of alloxan, ferritin immunostaining re-appeared in nuclei after the cells were returned to standard media (Figure 5B). If alloxan was present in the initial growth period, the reappearance of nuclear ferritin was inhibited, while cytoplasmic ferritin remained essentially unchanged. Adding iron (FAC) to the standard medium resulted in an approx. 200% increase in nuclear and cytoplasmic ferritin contents relative to levels found in untreated cells. However, the presence of alloxan in the FAC-supplemented medium blocked the increase in nuclear ferritin (Figure 5B) but not the increase of cytoplasmic ferritin (Figure 5C).

The effect of alloxan on ferritin redistribution is probably due to its influence on protein glycosylation or due to some other currently unknown effect. To demonstrate that alloxan inhibits O-glycosylation in SW1088 cell cultures, cells were treated with

Table 2 Putative O-glycosylation sites on H- and L-ferritin subunits

Predicted by http://www.cbs.dtu.dk/services/YinOYang/

Sequence	Residue result	*O*-GlcNAc	Potential threshold	Threshold (1)	Threshold (2)
H-ferritin	1 T	+++	0.5374	0.3210	0.3831
	2 T	+++	0.7013	0.3336	0.4000
	4 S	+++	0.7070	0.3357	0.4029
	5 T	++	0.5910	0.3643	0.4414
	6 S	++	0.4751	0.3778	0.4597
	178 S	+	0.3927	0.3202	0.3820
	182 S	+	0.3243	0.2905	0.3420
L-ferritin	1 S	++	0.4819	0.3371	0.4146
	2 S	+++	0.5466	0.3443	0.4048
	9 S	+	0.4223	0.3797	0.4622
	10 T	+	0.4564	0.3837	0.4676

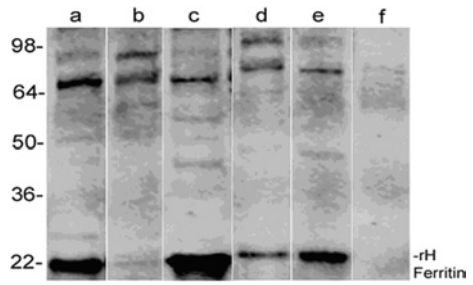

Figure 4 H-ferritin can be immunoprecipitated with a monoclonal antibody raised against GlcNAc

Astrocytoma (SW1088) cells were lysed. Cytoplasmic and nuclear fractions were isolated and 1 mg of total protein from each fraction was pretreated with Protein A/G to precipitate proteins with IgG-like folds. Supernatants were then treated with a monoclonal antibody raised against GlcNAc, and immunocomplexes were precipitated with additional Protein A/G. Precipitated immunocomplexes were subjected to SDS/PAGE and the blots were stained with anti-human H-ferritin polyclonal antibody as described in the Materials and methods section. Lane a, proteins precipitated from total nuclear extract with an antibody raised against *O*-GlcNac; lane b, nuclear extract proteins remaining in the supernatant after immunoprecipitation; lane c, proteins precipitated from cytoplasmic extract with an antibody raised against *O*-GlcNac; lane d, cytoplasmic proteins remaining in the supernatant after immunoprecipitation; lane e, total nuclear extract without immunoprecipitation (20 μg of protein was loaded for this sample); lane f, precipitate of anti-*O*-GlcNac antibody with Protein A/G (no cellular proteins). These results show that O-glycosylated ferritin is found in both the nucleus and cytoplasm. On the basis of densitometric analysis of the band intensity, the ratio of cytoplasmic to nuclear O-glycosylated ferritin is approx. 1.8:1. However, the total amount of ferritin in the cytoplasm is four to six times higher than that found in the nucleus. See the Discussion section for details.

0, 0.1, 0.5 and 1.0 mM alloxan for 96 h. The cells were then harvested and total soluble proteins were analysed by slot blot for O-glycosylation. The results are shown in Figure 6 and indicate that alloxan treatment decreases the total amount of O-glycosylated protein in a dose-dependent manner. The concentration of alloxan chosen did not affect cell viability (inset to Figure 6). Together, these results support the hypothesis that ferritin O-glycosylation and translocation into the nucleus are coupled processes.

Alloxan treatment does not induce iron release from ferritin

Sakurai and Miura [46,47] have shown that the combination of alloxan and glutathione can stimulate iron release from ferritin. To determine whether alloxan-induced iron release from ferritin is a possible explanation for the differences in ferritin translocation to the nucleus, evidence for alloxan-induced iron release was sought using the *in vitro* DNA supercoil-relaxation assay [19]. We have shown previously that iron released from ferritin rapidly nicks superhelical DNA and that this provides a sensitive assay for iron release [19]. Supercoil-relaxation assays were performed with the plasmid pUC 19 DNA incubated with ferritin in the presence of different concentrations of alloxan. Comparison of the time course of reactions run with rH-ferritin and rH-ferritin + alloxan shows that all reactions have a characteristic lag at early times, followed by an interval of increasing nicking activity (Figure 7). The duration of the lag phase and the steady-state nicking rates are similar for all reactions with or without alloxan present, strongly suggesting that, under our assay conditions, alloxan treatment does not effect the rate or amount of iron release from ferritin.

DISCUSSION

The sources, identities and functions of nuclear ferritins have been in question ever since their discovery. In the present study, we have shown that ferritin isolated from the nuclei of SW1088 astrocytoma cells shares many properties with cytoplasmic human H-ferritin, including mobility in SDS/PAGE, resistance to proteolysis and heat denaturation and reaction with polyclonal and monoclonal antibodies raised against the cytoplasmic form. Furthermore, siRNA directed against the mRNA-encoding cytoplasmic human H-ferritin [28] decreases the presence of ferritin in SW1088 nuclei in a transient manner (Figure 3A). Thus, unlike mitochondrial ferritin, which appears to be transcribed from a different gene [48], nuclear ferritin is translated from the same mRNA as cytoplasmic ferritin. The L-ferritin subunit was not detected in the nuclear fraction, consistent with previous publications on these cells from our laboratory [10] and also on other cell types by others [11,17,18]. What is the source of the nuclear protein? Initial studies have suggested that cytoplasmic ferritin diffuses into the cell nucleus, although the data of Feldherr and co-workers [49,50] suggested that the mature 24-mer assembly may be too large to make the transit intact. More recently, we have shown that ferritin can enter the nuclei through the nuclear pore [10]. Although this does not rule out that other pathways may operate in parallel, the simplest view and our current hypothesis is that ferritin molecules partition between cytoplasmic and nuclear pools in response to environmental and developmental cues.

What controls the distribution of H-ferritin between nuclear and cytoplasmic compartments? The lack of obvious nuclear localization sequences suggests that a different signal may regulate its translocation. One possibility is O-glycosylation [39–44]. Several studies have shown that monoclonal antibodies or lectins that bind *O*-GlcNAc block the nuclear transport of macromolecules at an energy-dependent step [51,52]. Consistent with this notion, we have previously shown that movement of ferritin into the nucleus is ATP-dependent and can be blocked by wheatgerm agglutinin [10]. A theoretical search for possible O-glycosylation sites revealed four high-probability sites located in the N-terminal end of the H-ferritin sequence (Table 2) that are not present in the L-ferritin primary sequence (Figure 8). Only one site was predicted for L-ferritin (Table 2). The prediction that H-ferritin is O-glycosylated is supported experimentally: ferritin was efficiently immunoprecipitated from nuclear and cytoplasmic fractions with antibodies raised against *O*-GlcNAc (Figure 4).

The difference in the number and location of potential O-glycosylation sites between H- and L-ferritin suggests a rationale for the preferential nuclear uptake of H-ferritin [8,10,17]. Our results indicate that total ferritin is distributed between the cytoplasm and nucleus in a 6:1 molar ratio, but the ratio is decreased more than 3-fold (1.8:1) when the relative amounts of O-glycosylated ferritin are considered (Figure 4). These results suggest that the molar ratio of ferritin that is O-glycosylated is much higher in the nucleus than in the cytoplasm, consistent with the notion that O-glycosylation is necessary for H-ferritin transfer to the nucleus.

Treatment of cells with alloxan has been used to block O-glycosylation [45]. Treatment of SW1088 cells with alloxan decreases the glycosylation of soluble proteins without significant effects on cell viability and blocks the DFO-dependent translocation of ferritin from the cytoplasm to the nucleus. This effect is amplified when cells are grown in the presence of FAC, which significantly increases the nuclear ferritin content (Figures 5 and 6). Taken together, these results suggest that glycosylation plays an important role in ferritin translocation. However, at present, we do not know whether alloxan exerts its effect on translocation by blocking ferritin glycosylation or by inhibiting the glycosylation of some other component that is essential for ferritin translocation (e.g. a subunit of the nuclear pore complex). In view of these effects, it is intriguing that alloxan does not prevent the disappearance of ferritin from the nuclear fraction when DFO is added. This result indicates that the effect of alloxan on the

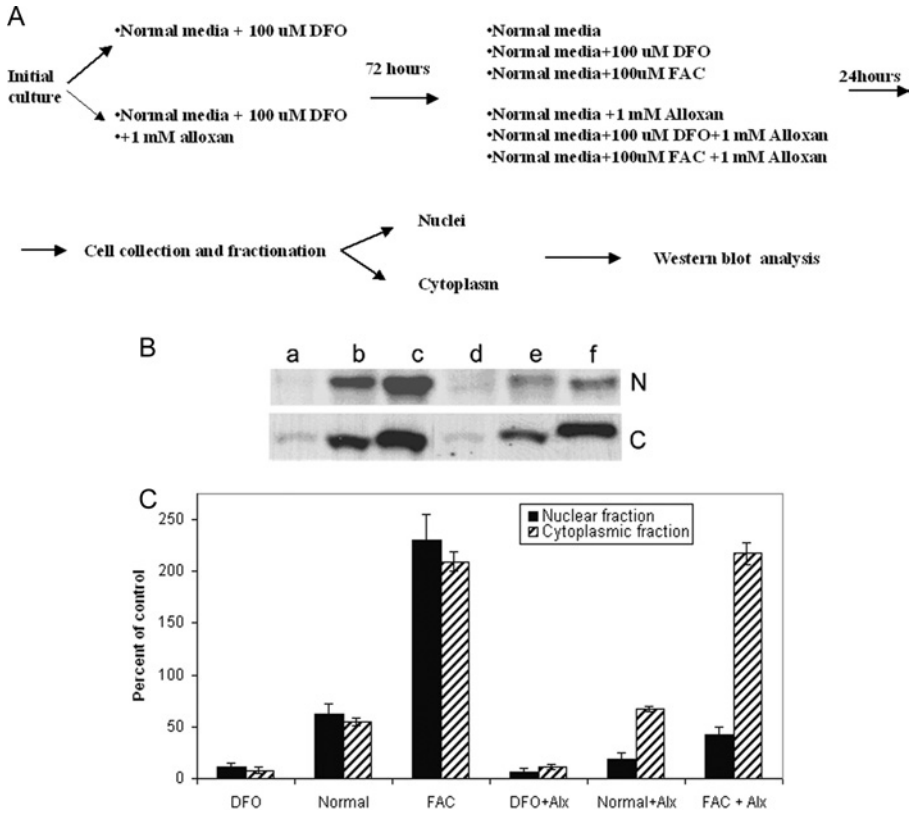

Figure 5 Nuclear import of ferritin is inhibited by alloxan, whereas cytoplasmic levels of ferritin are not affected

Under resting conditions, SW1088 cells contain ferritin in both nuclear and cytoplasmic compartments. Treatment of cells with the iron chelator DFO significantly decreases ferritin content in both compartments. The reappearance of ferritin in cytoplasmic and nuclear compartments after DFO treatment (alone) or treatment with DFO + alloxan is affected by the presence of alloxan (alx) and/or FAC in the culture medium. (**A**) Diagram of the experimental procedure, showing the time course of changes in culture conditions. (**B**) Western blots of nuclear (N) and cytoplasmic (C) extracts of SW1088 cells, resolved by SDS/PAGE. Samples of the nuclear extract contained 20 μg of total protein, whereas samples of the cytoplasmic extract contained 10 μM of total protein. Ferritin was detected with HS-59 mouse monoclonal antibody and horseradish peroxidase-conjugated goat anti-mouse IgG, as described in the Materials and methods section. Lane a, extracts from cells cultured in medium containing 100 μM DFO; lane b, extracts of cells cultured in normal medium; lane c, extracts of cells cultured in 100 μM FAC; lane d, extracts of cells cultured in 100 μM DFO + 1 mM alloxan; lane e, extracts of cells cultured in normal medium supplemented with 1 mM alloxan; lane f, extracts of cells cultured in medium supplemented with 100 μM FAC + 1 mM alloxan. (**C**) Summary of ferritin contents. The relative amounts of ferritin in the nuclear (black bars) and cytoplasmic (striped bars) fractions were measured after an initial treatment with DFO alone or DFO + 100 μM alloxan and a subsequent culture in the presence of DFO alone, normal medium, medium supplemented with FAC, medium supplemented with DFO + alloxan, normal medium + alloxan or normal medium + FAC and alloxan. The relative amounts of ferritin are normalized to the amount of ferritin in the corresponding fractions before the initial DFO treatment.

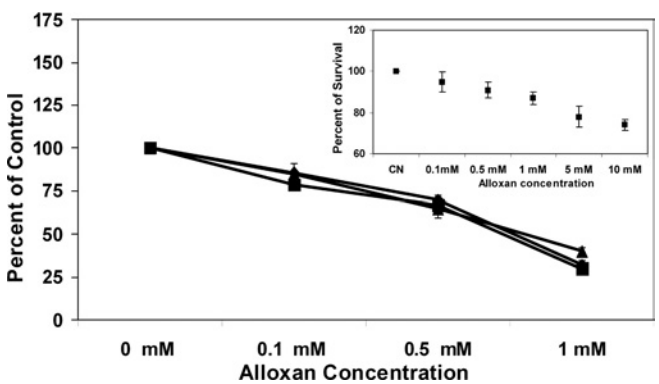

Figure 6 Alloxan inhibits protein O-glycosylation in SW1088 human astrocytoma cells

Cells were grown in triplicate independent cultures in the presence of 0, 100, 500 μM and 1 mM concentrations of alloxan as described in the Materials and methods section. Aliquots of whole cell lysates from each culture were applied to a nitrocellulose membrane using a vacuum slot blot device. The membrane was blocked in a 5 % solution of non-fat dry milk at 21 $\pm$ 1 °C for 1 h and incubated overnight with mouse monoclonal anti-*O*-GlcNAc antibody. Immunocomplexes were detected and quantified as described in the Materials and methods section. As an internal control for this assay, membrane loadings of 1 (◆), 5 (■) and 10 (▲) μg of total protein were tested and they gave similar responses to changes in the concentration of alloxan in the original cultures. The results show that less O-glycosylated protein is available for detection as [alloxan] increases; parallel testing for cell viability with MTT (inset) shows that, at 1 mM alloxan (the concentration chosen for the study of ferritin translocation), 87 $\pm$ 3 % of the cells remain viable.

concentration of ferritin in the nucleus is asymmetric: it inhibits ferritin uptake but not its removal.

Alloxan had no effect on the reappearance of ferritin in cytoplasmic fractions when DFO-treated cells were returned to normal medium. The presence of FAC in the growth medium did not change this outcome even though cells contained approx. two times more ferritin when cultured with this iron source than when grown in its absence. In contrast with the trend seen with nuclear fractions, the presence of alloxan had no detectable effect on the ferritin content of cytoplasmic fractions. Together, these results indicate that alloxan treatment has little or no effect on the synthesis of detectable, cytoplasmic H-ferritin species or on the depletion of ferritin from the cytoplasm in the presence of strong chelators such as DFO.

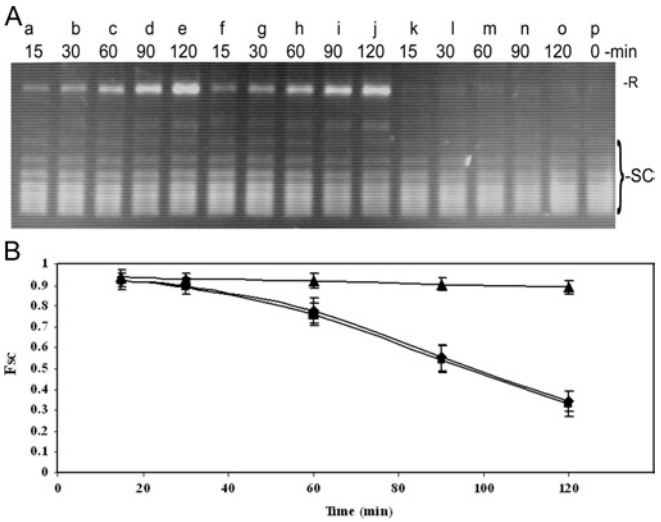

Figure 7 Treatment with alloxan does not cause iron-release from ferritin *in vitro*

Supercoil-relaxation assays were performed with pUC19 plasmid DNA (0.5 μg/assay) as described in the Materials and methods section. (**A**) Electrophoretic profiles of pUC19 DNA incubated in the presence of recombinant H-ferritin (lanes a–e), recombinant H-ferritin + 1 mM alloxan (lanes f–j) and 1 mM alloxan alone (lanes k–o). Reaction times were as indicated. Lane p, a sample of the superhelical pUC19 DNA that was not treated with ferritin. Band assignments: R, relaxed circle form; SC, superhelical topoisomers. (**B**) Graph of the mole fraction of superhelical DNA as a function of the reaction time for samples containing rH-ferritin (◆), rH-ferritin + 1 mM alloxan (■) and 1 mM alloxan alone (▲). Data were obtained from three experiments similar to that shown in (**A**). Error bars represent S.D. values. Similar rates of DNA relaxation by ferritin both in the presence and absence of alloxan indicate that alloxan does not cause a significant release of iron from ferritin under these conditions.

```
H-ferritin_
TTASTSQVRQNYHQDSEAAINRQINLELYASYVYLSMSYYFDRDDVALKNFAKYFLHQSH
L-ferritin_       ----
SSQIRQNYSTDVEAAVNSLVNLYLQASYTYLSLGFYFDRDDVALEGVSHFFRELAE


H-ferritin_
EEREHAEKLMKLQNQRGGRIFLQDIKKPDCDDWESGLNAMECALHLEKNVNQSLLELHKL
L-ferritin_
EKREGYERLLKMQNQRGGRALFQDIKKPAEDEWGKTPDAMKAAMALEKKLNQALLDLHAL


H-ferritin_
ATDKNDPHLCDFIETHYLNEQVKAIKELGDHVTNLRKMGAPESGLAEYLFDKHTLGDSDN
L-ferritin_
GSARTDPHLCDFLETHFLDEEVKLIKKMGDHLTNLHRLGGPEAGLGEYLFERLTLKHD--


H-ferritin_       ES
L-ferritin_       --
```

Figure 8 H- and L-ferritin sequence alignment

The high potential O-glycosylation sites in H-ferritin (shown in boldface and underlined) are found in the N-terminal sequence in a location that does not overlap the L-ferritin sequence. Low probability sites in H-ferritin (shown in boldface, underlined and italicized) also are not found in overlapping regions of the L-ferritin sequence at the C-terminal end.

Confocal microscopy performed on the immunohistochemically stained cells reveals a heterogeneous distribution of ferritin within the nuclei of SW1088 cells (Figure 1). A similar 'speckled' appearance has been reported for ferritin in the nuclei of K562 cells [38]. Together, these results suggest that ferritin is concentrated in specific nuclear volumes (as distinct from a uniform distribution). At present, our results do not allow us to distinguish between models in which ferritin is associated with one or more components that form foci and models in which ferritin passively occupies volumes around and between other nuclear structures. Both models are consistent with the 'punctate' or 'granular' distributions of ferritin that we observe (Figure 1) and both are compatible with the non-random association of ferritin with different nuclear fractions (Figure 2A). At present, we do not know whether this pattern will extend to all other cell types.

In the course of this work, a number of questions have arisen that call for further investigation. Perhaps the most important of these is the role of post-translational modification in ferritin translocation and in its turnover. Similarly, we would like to know with what molecular systems does ferritin associate during the translocation process and how is the process regulated. Finally, the fact that ferritin appears in the nucleus in response to environmental signals suggests that it plays a functional role in that compartment. The increasing content of ferritin in the soluble chromatin when compared with the nuclear matrix or nucleolar fractions leads us to speculate that ferritin may specifically bind some component of heterochromatin. If this is the case, we anticipate a functional role for ferritin, perhaps in iron sequestration or delivery, in the molecular transactions of chromatin.

This work was supported by a grant from the National Institutes of Health (DK54289). We are grateful to Dr P. Arosio for helpful discussions.

REFERENCES

1 Kwok, J. C. and Richardson, D. R. (2004) Examination of the mechanism(s) involved in doxorubicin-mediated iron accumulation in ferritin: studies using metabolic inhibitors, protein synthesis inhibitors, and lysosomotropic agents. Mol. Pharmacol. **65**, 181–195
2 Harrison, P. M. and Arosio, P. (1996) The ferritins: molecular properties, iron storage function and cellular regulation. Biochim. Biophys. Acta **1275**, 161–203
3 Haddow, A. and Horning, E. S. (1960) On the carcinogenicity of an iron dextran complex. J. Natl. Cancer Inst. **24**, 109–147
4 Smith, A. G., Carthew, P., Francis, J. E., Edwards, R. E. and Dinsdale, D. (1990) Characterization and accumulation of ferritin in hepatocyte nuclei of mice with iron overload. Hepatology **12**, 1399–1405
5 Iancu, T. C., Rabinowitz, H., Brissot, P., Guillouzo, A., Deugnier, Y. and Bourel, M. (1985) Iron overload of the liver in the baboon. An ultrastructural study. J. Hepatol. **1**, 261–275
6 Shires, T. K. (1982) Iron-induced DNA damage and synthesis in isolated rat liver nuclei. Biochem. J. **205**, 321–329
7 Vaca, C. E. and Harms-Ringdahl, M. (1989) Interaction of lipid peroxidation products with nuclear macromolecules. Biochim. Biophys. Acta **1001**, 35–43
8 Cai, C. X., Birk, D. E. and Linsenmayer, T. F. (1998) Nuclear ferritin protects DNA from UV damage in corneal epithelial cells. Mol. Biol. Cell **9**, 1037–1051
9 Beard, J. L., Connor, J. D. and Jones, B. C. (1993) Brain iron: location and function. Prog. Food Nutr. Sci. **17**, 183–221
10 Thompson, K. J., Fried, M. G., Ye, Z., Boyer, P. and Connor, J. R. (2002) Regulation, mechanisms and proposed function of ferritin translocation to cell nuclei. J. Cell Sci. **115**, 2165–2177
11 Cai, C. X., Birk, D. E. and Linsenmayer, T. F. (1997) Ferritin is a developmentally regulated nuclear protein of avian corneal epithelial cells. J. Biol. Chem. **272**, 12831–12839
12 Blissman, G., Menzies, S., Beard, J., Palmer, C. and Connor, J. R. (1996) The expression of ferritin subunits and iron in oligodendrocytes in neonatal porcine brains. Dev. Neurosci. **18**, 274–281
13 Cheepsunthorn, P., Palmer, C. and Connor, J. R. (1998) Cellular distribution of ferritin subunits in postnatal rat brain. J. Comp. Neurol. **400**, 73–86
14 Cheepsunthorn, P., Palmer, C., Menzies, S., Roberts, R. L. and Connor, J. R. (2001) Hypoxic/ischemic insult alters ferritin expression and myelination in neonatal rat brains. J. Comp. Neurol. **431**, 382–396
15 Cheepsunthorn, P., Radov, L., Menzies, S., Reid, J. and Connor, J. R. (2001) Characterization of a novel brain-derived microglial cell line isolated from neonatal rat brain. Glia **35**, 53–62

16 Lanford, R. E., Kanda, P. and Kennedy, R. C. (1986) Induction of nuclear transport with a synthetic peptide homologous to the SV40 T antigen transport signal. Cell (Cambridge, Mass.) **46**, 575–582
17 Cai, C. X. and Linsenmayer, T. F. (2001) Nuclear translocation of ferritin in corneal epithelial cells. J. Cell Sci. **114**, 2327–2334
18 Millholland, J. M., Fitch, J. M., Cai, C. X., Gibney, E. P., Beazley, K. E. and Linsenmayer, T. F. (2003) Ferritoid, a tissue-specific nuclear transport protein for ferritin in corneal epithelial cells. J. Biol. Chem. **278**, 23963–23970
19 Surguladze, N., Thompson, K. M., Beard, J. L., Connor, J. R. and Fried, M. G. (2004) Interactions and reactions of ferritin with DNA. J. Biol. Chem. **279**, 14694–14702
20 Stacey, D. W. and Allfrey, V. G. (1984) Microinjection studies of protein transit across the nuclear envelope of human cells. Exp. Cell Res. **154**, 283–292
21 Benkovic, S. A. and Connor, J. R. (1993) Ferritin, transferrin, and iron in selected regions of the adult and aged rat brain. J. Comp. Neurol. **338**, 97–113
22 Poss, K. D. and Tonegawa, S. (1997) Heme oxygenase 1 is required for mammalian iron reutilization. Proc. Natl. Acad. Sci. U.S.A. **94**, 10919–10924
23 Broyles, R. H., Blair, F. C., Kyker, K. D., Kurein, B. T., Stewart, D. R., Hala'sz, H., Berg, P. E. and Schechter, A. N. (1995) A ferritin-like protein binds to a highly conserved CAGTGC sequence in the beta-globin promoter. In Sickle Cell Disease and Thalassamias: New Trends in Therapy (Beuzard, Y., Lubin, B. and Rosa, J., eds.), pp. 43–51, Colloque INSERM/John Libbey Eurotext Ltd, Paris
24 Hurta, R. A. and Wright, J. A. (1991) Correlation between levels of ferritin and the iron-containing component of ribonucleotide reductase in hydroxyurea-sensitive, -resistant, and -revertant cell lines. Biochem. Cell Biol. **69**, 635–642
25 Mosmann, T. (1983) Rapid colorimetric assay for cellular growth and survival: application to proliferation and cytotoxicity assays. J. Immunol. Methods **65**, 55–63
26 Graham, J. M. (1993) The identification of subcellular fractions from mammalian cells. Methods Mol. Biol. **19**, 1–18
27 Bush, E. (1967) Nucleic acids. In Methods in Enzymology, vol. 12 (Grossman, L. and Moldave, K., eds.), pp. 448–464, Academic Press, New York
28 Cozzi, A., Corsi, B., Levi, S., Santambrogio, P., Biasiotto, G. and Arosio, P. (2004) Analysis of the biologic functions of H- and L-ferritins in HeLa cells by transfection with siRNAs and cDNAs: evidence for a proliferative role of L-ferritin. Blood **103**, 2377–2283
29 Cavanna, F., Ruggeri, G., Iacobello, C., Chieregatti, G., Murador, E., Albertini, A. and Arosio, P. (1983) Development of a monoclonal antibody against human heart ferritin and its application in an immunoradiometric assay. Clin. Chim. Acta **134**, 347–356
30 Cavanna, F., Ruggeri, G., Chieregatti, G., Murador, E., Arosio, P. and Albertini, A. (1984) Evaluation of heart isoferritins in serum using specific monoclonal antibodies. Ric. Clin. Lab. **14**, 337–340
31 Luzzago, A., Arosio, P., Iacobello, C., Ruggeri, G., Capucci, L., Brocchi, E., De Simone, F., Gamba, D., Gabri, E. and Levi, S. (1986) Immunochemical characterization of human liver and heart ferritins with monoclonal antibodies. Biochim. Biophys. Acta **872**, 61–71
32 Cazzola, M., Arosio, P., Bellotti, V., Bergamaschi, G., Dezza, L., Iacobello, C. and Ruggeri, G. (1985) Use of a monoclonal antibody against human heart ferritin for evaluating acidic ferritin concentration in human serum. Br. J. Haematol. **61**, 445–453
33 Henderson, R. J. and Connor, J. R. (2005) Development of a fluorescent reporter to assess iron regulatory protein activity in living cells. Biochim. Biophys. Acta **1743**, 162–168
34 Bittman, K. (2004) Mean Pixel Density Analysis of ImagePro Software for Fluorescent Quantitation. Phase 3 Imaging, Glen Mills, PA
35 Tachon, P. (1989) Ferric and cupric ions requirement for DNA single-strand breakage by H_2O_2. Free Radical Res. Commun. **7**, 1–10
36 Crowe, A. and Morgan, E. H. (1992) Iron and transferrin uptake by brain and cerebrospinal fluid in the rat. Brain Res. **592**, 8–16
37 Henle, E. S., Luo, Y., Gassmann, W. and Linn, S. (1996) Oxidative damage to DNA constituents by iron-mediated Fenton reactions. The deoxyguanosine family. J. Biol. Chem. **271**, 21177–21186
38 Pountney, D., Trugnan, G., Bourgeois, M. and Beaumont, C. (1999) The identification of ferritin in the nucleus of K562 cells, and investigation of a possible role in the transcriptional regulation of adult beta-globin gene expression. J. Cell Sci. **112**, 825–831
39 Comer, F. I. and Hart, G. W. (2000) O-glycosylation of nuclear and cytosolic proteins. Dynamic interplay between O-GlcNAc and O-phosphate. J. Biol. Chem. **275**, 29179–29182
40 Vosseller, K., Wells, L. and Hart, G. W. (2001) Nucleocytoplasmic O-glycosylation: O-GlcNAc and functional proteomics. Biochimie **83**, 575–581
41 Wells, L., Wells, L., Gao, Y., Mahoney, J. A., Vosseller, K., Chen, C., Rosen, A. and Hart, G. W. (2002) Dynamic O-glycosylation of nuclear and cytosolic proteins: further characterization of the nucleocytoplasmic beta-N-acetylglucosaminidase, O-GlcNAcase. J. Biol. Chem. **277**, 1755–1761
42 Wells, L. and Hart, G. W. (2003) O-GlcNAc turns twenty: functional implications for post-translational modification of nuclear and cytosolic proteins with a sugar. FEBS Lett. **546**, 154–158
43 Jentoft, N. (1990) Why are proteins O-glycosylated? Trends Biochem. Sci. **15**, 291–294
44 Ernst, J. F. and Prill, S. K. (2001) O-glycosylation. Med. Mycol. **39** (Suppl. 1), 67–74
45 Konrad, R. J., Zhang, F., Hale, J. E., Knierman, M. D., Becker, G. W. and Kudlow, J. E. (2002) Alloxan is an inhibitor of the enzyme O-linked N-acetylglucosamine transferase. Biochem. Biophys. Res. Commun. **293**, 207–212
46 Sakurai, K. and Miura, T. (1988) Iron release from ferritin and generation of hydroxyl radical in the reaction system of alloxan with reduced glutathione; a role of ferritin in alloxan toxicity. Chem. Pharm. Bull. (Tokyo) **36**, 4534–4538
47 Miura, T. and Sakurai, K. (1988) Iron release from ferritin by alloxan radical. Life Sci. **43**, 2145–2149
48 Levi, S. and Arosio, P. (2004) Mitochondrial ferritin. Int. J. Biochem. Cell Biol. **36**, 1887–1889
49 Paine, P. L. and Feldherr, C. M. (1972) Nucleocytoplasmic exchange of macromolecules. Exp. Cell Res. **74**, 81–98
50 Feldherr, C. M. (1962) The intracellular distribution of ferritin following microinjection. J. Cell Biol. **12**, 159–167
51 Turner, J. R., Tartakoff, A. M. and Greenspan, N. S. (1990) Cytological assessment of nuclear and cytoplasmic O-linked N-acetylglucosamine distribution by using anti-streptococcal monoclonal antibodies. Proc. Natl. Acad. Sci. U.S.A. **87**, 5608–5612
52 Comer, F. I., Vosseller, K., Wells, L., Accavitti, M. A. and Hart, G. W. (2001) Characterization of a mouse monoclonal antibody specific for O-linked N-acetylglucosamine. Anal. Biochem. **293**, 169–177

Received 5 November 2004/4 January 2005; accepted 27 January 2005
Published as BJ Immediate Publication 27 January 2005, DOI 10.1042/BJ20041853